Electronic Supplementary Material (ESI) for Physical Chemistry Chemical Physics.

SUPPLEMENTARY INFORMATION

Sub-molecular spectroscopy and temporary molecular charging of Ni-Phthalocyanine on graphene with STM

Mali Zhao[1], Faisal Almarzouqi[1†], Eric Duverger[2], Philippe Sonnet[3], Gérald Dujardin[1], Andrew J. Mayne[1*]

[1]Institut des Sciences Moléculaires d'Orsay, CNRS UMR 8214, Université Paris-Sud, Université Paris-Saclay, 91405 Orsay, France

[2]Institut FEMTO-ST, Université de Franche-Comté, CNRS UMR 6174, 15B avenue des Montboucons, F-25030, Besançon, France

[3]Institut de Science des Matériaux de Mulhouse IS2M, CNRS UMR 7361, Université de Haute Alsace, 3 bis rue Alfred Werner, 68093 Mulhouse, France

†present address: Department of Chemistry, Sultan Qaboos University, Muscat, Oman

*corresponding author: andrew.mayne@u-psud.fr

S1. Computational details

In order to investigate the electronic and molecular structure of the self-assembled layer of NiPc molecules on graphene, periodic Kohn-Sham DFT calculations using the VASP code were carried out [1, 2].The electron-electron exchange-correlation interactions were described by the function of Perdew, Burke, and Ernzerhof within the generalized gradient approximation (GGA) [3]. The projector augmented wave method was used to describe the electron-ion interactions [4, 5]. A plane wave basis set with an energy cutoff of 400 eV was used. In order to take into account the experimental molecule-molecule distances in the NiPc lattice and the steric hindrance between NiPc molecules, different multiple periodicities of the graphene surface were tested up to 15×15 with respect to the 1×1 graphene unit cell. As mentioned by Gao et al, the best adsorption energy of phthalocyanine on monolayer graphene (MLG) is obtained with the molecule centered on the top site [6].Thus, in these calculations each NiPc molecule center was initially positioned on top sites before relaxation of the full system.

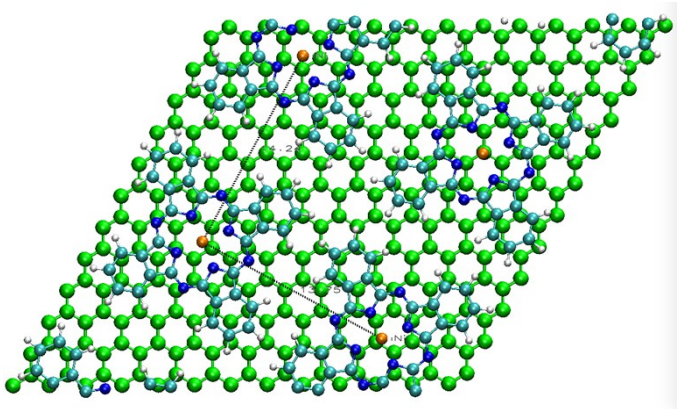

Figure S1. Supercell lattice used in the DFT calculations. The carbon atoms of the graphene are shown in green, the carbon atoms of the molecules are in turquoise, the nitrogen atoms in blue, the hydrogen atoms in white, and the Ni atoms in orange. The 13x12 unit cell is indicated by the dotted lines.

The Brillouin zones were sampled using a single k-point at the gamma point, which was a reasonable choice given the large size of the supercell employed (31.87Å×29.42Å×40Å for 13×12

with respect to the 1×1 graphene unit cell). In Figure S1, the model presented contains 852 atoms (624 atoms of C for the graphene and 228 atoms for the 4 molecules). The ionic structure was relaxed until all the components of the force acting on each atom were< 0.01 eV/Å. The dispersive interactions in the total energy calculations were included using the DFT-D3 approach to add the energetic correction term proposed by Grimme [6-8]. To characterize the molecule-surface interaction, the charge transfer was analyzed using a partial charge approach (i.e., the valence electrons) through the Bader scheme [9].

The STM images were calculated by feeding the relaxed atom positions obtained from the VASP code into the bSKAN code [10], which was designed to describe electron transport through a vacuum barrier. The theoretical model was based on multiple-scattering theory [11]. A pyramidal tip comprising 82 tungsten atoms, terminated by a single atom was employed to simulate the STM images.

S2. Orientations of NiPc molecular array on MLG/6H-SiC(0001).

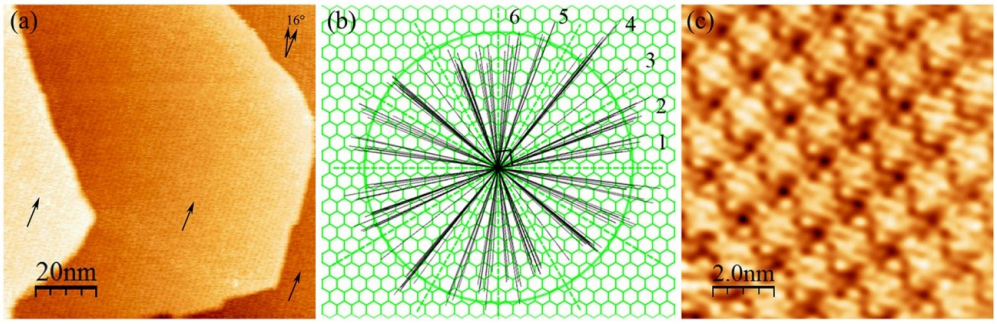

Figure S2. (a) 100nm×100nm STM image of self-assembled NiPc molecules on MLG/SiC(0001), tunneling condition: V = -2.5 V, I = 0.1 nA. NiPc molecules grow seamlessly across the surface steps between the left and middle graphene terraces. However, the molecular array direction in the upper right molecular terrace shows a 16° difference with that on the other molecular terraces; (b) The NiPc molecular lattice directions on MLG/SiC(0001) from the experiment are summarized by the grey-black solid lines for each molecular array. Every pair of orthogonal groups are tied to one molecular lattice direction, the angle difference between the adjacent molecular lattice directions is about 15°; (c) 10nm×10nm topography of empty NiPc molecular states, tunneling conditions: V = +1.6 V, I = 0.4 nA. The image was Fourier filtered to reduce the noise.

Statistically, the NiPc molecular network on graphene displays twelve molecular array directions (six molecular lattice directions) in total. The directions of the molecular array with respect to the underlying graphene are summarized by the grey-black lines in Figure S2 (b). Each pair of orthogonal arrays corresponds to one square lattice of the self-assembled molecular network. The twelve molecular array directions are distributed uniformly on the graphene with an average angle of 15° (±2°), which is the half of the angle between the adjacent armchair and zigzag directions of graphene. For MLG, C-C bonds have a three-fold symmetry, whereas the NiPc molecule has D_{4h} symmetry. The twelve NiPc molecular array directions can be deduced as the combination of C-C crystallographic directions of the graphene with four molecular conformations. This confirms the molecular lattice is commensurate with the graphene substrate (carpet-like molecular network across graphene step in Figure S2). Therefore, the molecular lattice directions are governed by the symmetry of both substrate (graphene) and molecule.

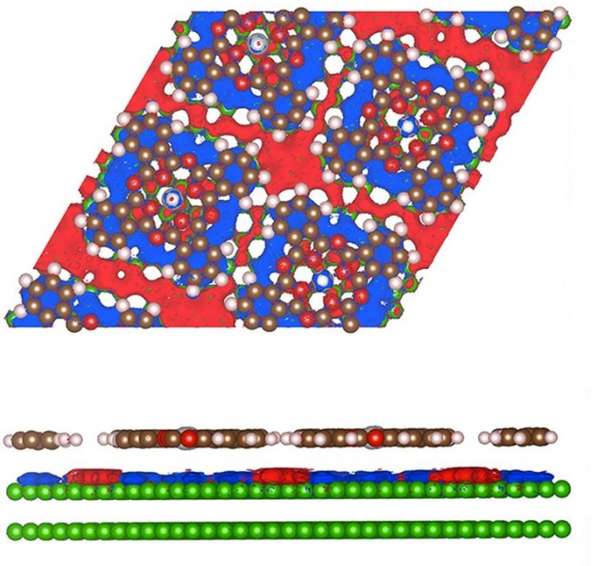

Figure S3. The calculation of the charge differences for the n-doped system was performed. The figure shows the side and top view, respectively. The red and blue colors correspond to an augmentation and a diminution of the electron density, respectively. Only the top layer of graphene is affected by the presence of the molecular layer (side view). Below the molecules, we observe a clear diminution of the electron density (top view). The top C layer is decoupled from the bottom C layer Therefore, these calculations enable us to

consider that the top layer of the graphene is equivalent to the GML while the bottom layer (considered as fixed in the calculations) is equivalent to the buffer layer.

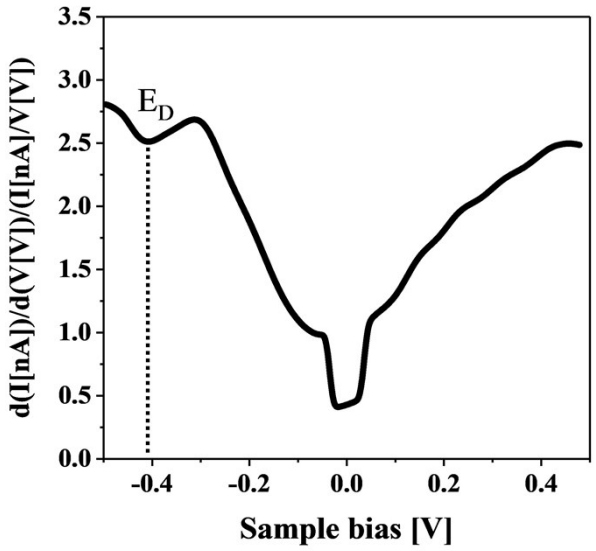

Figure S4. NDC curves for MLG (MLG)/SiC(0001) before molecular deposition. MLG shows a 0.07 eV gap-like feature and the Dirac point of MLG is 0.41 eV below the Fermi level.

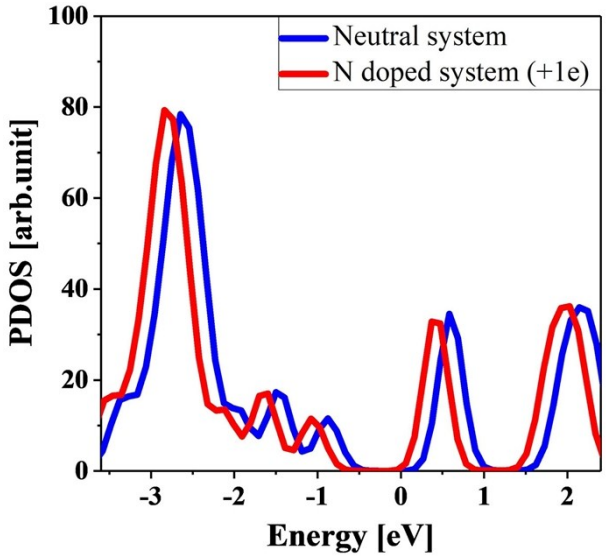

Figure S5. The PDOS of the molecule is presented with respect to the energy (0 corresponds to the Fermi level position for the two cases) in the neutral and n-doped system (blue and red curves, respectively).

The projected density of states (PDOS) of the NiPc molecules adsorbed on AA-stacked bilayer graphene (BLG) was calculated. The data was obtained for four self-assembled NiPc molecules adsorbed on the AA-stacked BLG. For each molecular orbital, the energy with respect to the Fermi level is given, along with the contribution of each atom (Ni, N, and C) to the PDOS. The values are presented in Table S1 and the spatial plots in Figure S6.

	HOMO-3	HOMO-2	HOMO-1	HOMO	LUMO	LUMO+1
Molecular Orbital (eV)/neutral case	-2.56	-1.90	-1.46	-0.86	+0.6	+2.17
Molecular Orbital (eV)/one charge case	-2.73	-2.11	-1.69	-1.07	+0.37	+2.02
Ni (%)	4.0	9.7	43.8	0	8.8	0.4
N (%)	47.1	68.3	16.9	3.5	41.8	19.3
C (π) (%)	48.9	22.1	39.2	96.5	49.4	80.3

Table S1. For each molecular orbital, the energy with respect to the Fermi level is given, along with the percentage contribution of each atom (Ni, N, and C) to the PDOS.

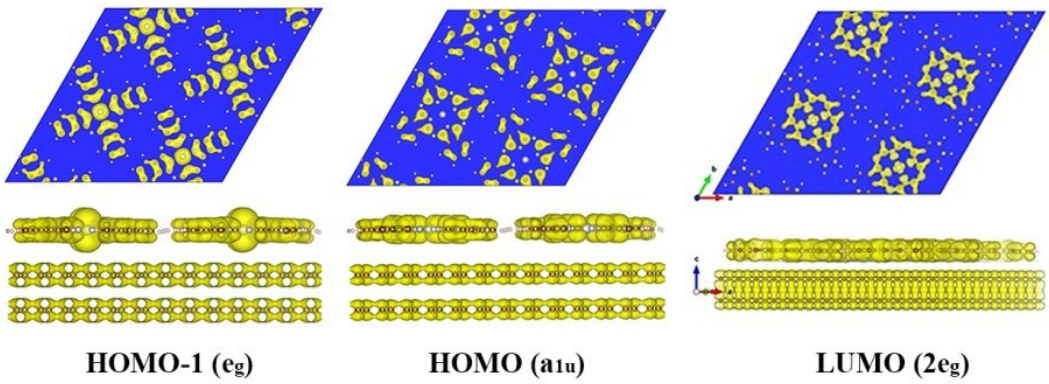

Figure S6. The calculated spatial charge distribution for each PDOS peak of the self-assembled NiPc molecules on AA-stacked BLG. The symmetries of HOMO-1, HOMO and LUMO are e_g, a_{1u} and $2e_g$ respectively. The charge transfer is close to zero between the NiPc molecular layer and the graphene.

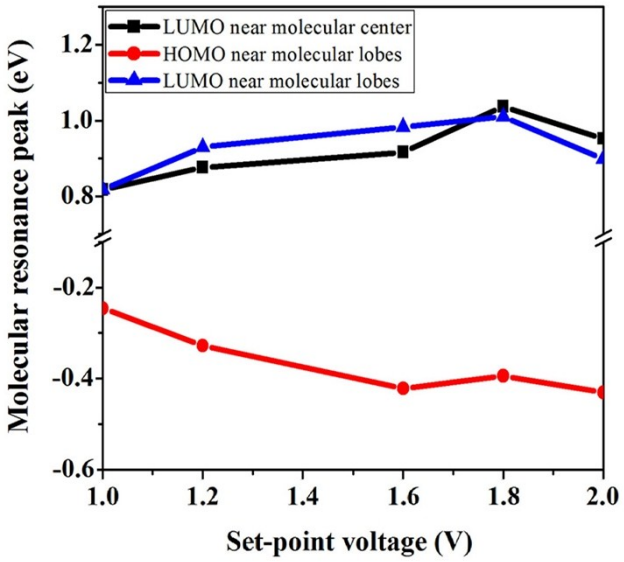

Figure S7. Molecular resonance peaks shift as a function of the set-point voltage. As the set-point voltage varies from +2.0 V to +1.0 V, the HOMO peak shifts 0.19 eV monotonously towards the Fermi level, while from the set-point voltage of +2.0V to +1.8V, the LUMO peak shifts from +0.89eV to +1.01eV, and then when the set-point voltage decreases further to +1.0V, the LUMO peak shifts 0.22eV monotonously to the Fermi level.

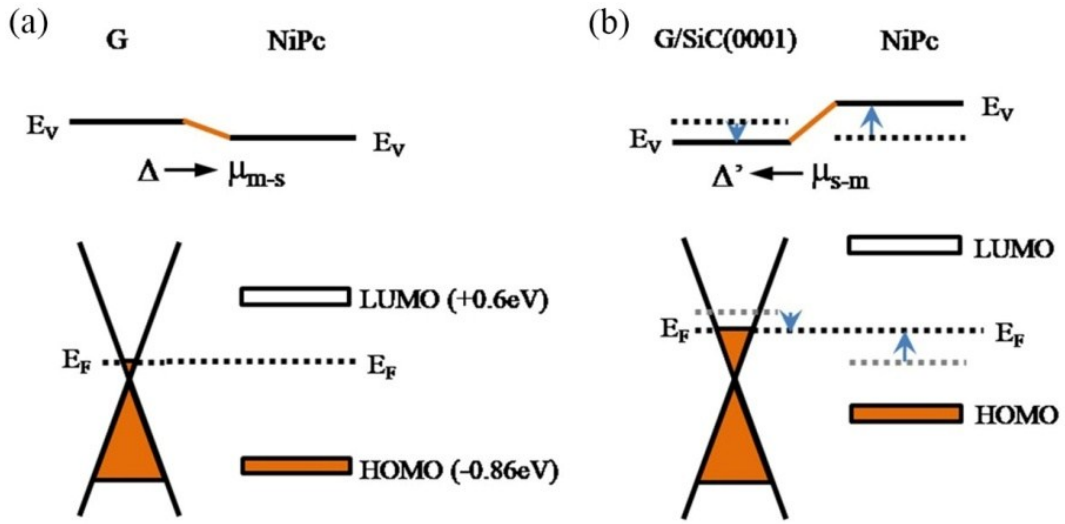

Figure S8. (a) Energy level alignment at the interface between NiPc molecules and free-standing AA-stacked BLG; (b) Energy level alignment at the interface between NiPc molecules and MLG on SiC (0001).

REFERENCES

[1] Kresse G., and Hafner J. Ab initio molecular dynamics for liquid metals. *Phys. Rev. B.***1993**,47, 222-229.

[2] Kresse G., and Furthmüller J. Efficient iterative schemes for ab initio total-energy calculations using a plane-wave basis set. *Phys. Rev. B.***1996**, 54, 11169-11186.

[3] Perdew J. P., Burke K., and Ernzerhof M. Generalized gradient approximation made simple. *Phys. Rev. Lett.***1996**, 77, 3865-3868.

[4] Blöchl P. E. Projector augmented-wave method. *Phys. Rev. B.***1994**, 50, 17953- 17979.

[5] Kresse G., and Joubert D. From ultrasoft pseudopotentials to the projector augmented-wave method. *Phys. Rev. B.***1999**, 59, 1758-1775.

[6] Grimme S. Accurate description of van der Waals complexes by density functional theory including empirical corrections. *J Comput Chem.***2004**, 25, 1463-1473.

[7] Grimme S. Semiempirical GGA-type density functional constructed with a long-range dispersion correction. *J Comput Chem.***2006**, 30, 1787-1799.

[8] Grimme S., Antony J., and Schwabe T.*, et al.* Density functional theory with dispersion corrections for supramolecular structures, aggregates, and complexes of (bio)organic molecules. *Org. Biomol. Chem.***2007**, 5, 741-758.

[9] Henkelman G., Arnaldsson A., and Jónsson H. A fast and robust algorithm for Bader decomposition of charge density. *Comput. Mater. Sci.* **2006**, 36, 354-360.

[10] Hofer W. A. Challenges and errors: interpreting high resolution images in scanning tunneling microscopy. *Prog. Surf. Sci.***2003**, 71, 147-183.

[11] Palotás K., and Hofer W. A. Multiple scattering in a vacuum barrier obtained from real-space wavefunctions. *J. Phys. Condens. Matter.***2005**, 17, 2705-2713.